

Laser Interaction with ZnO Nanostructure Enhanced by Microwave Plasma

Noori S. Anad, Gamal Abdel Fattah*, Khaled A. Elsayed, and Lotfi Z. Ismail**

Department of Physics, Faculty of science, Cairo University, Egypt

* Laser science and Interaction Department National Institute of Laser Enhanced science (NILES).

Lotfizaki@hotmail.com

Abstract: Pulsed Nd: YAG laser interaction with ZnO nanostructure have been carried out using both X-ray Diffraction (XRD) and Scanning Electron Microscopy (SEM). The applied ZnO nanostructure have been grown applying Microwave power enhanced chemical vapor deposition (MPECVD). The radiated sample started with hexagonal crystalline structure. The particle size equals 60 - 70 nm. The laser radiation reduced the particle size to be in the range 30-40 nm and the nanotube coupling have been changed to orthogonal structure with clear connecting centers. By increasing the laser shots the morphology of the nanostructure replaced by a mish shape with a reduction of the crystalline planes.

[Noori S. Anad, Gamal Abdel Fattah, Khaled A. Elsayed, and Lotfi Z. Ismail. **Laser Interaction with ZnO Nanostructure Enhanced by Microwave Plasma**. *N Y Sci J* 2012;5(12):137-142]. (ISSN: 1554-0200). <http://www.sciencepub.net/newyork>. 20

Keyword: ZnO nanostructure, MPECVD, Laser interaction, nano-tubes

1. Introduction:

Laser pulse interactions with matter are leading to various permanent surfaces morphology special attentions have been given for synthesizing nanostructure materials has been investigating [1-8]. Different modifications interaction mechanisms have been suggested for ultrafast laser interaction. Also the laser parameters such as flounce, number of shot gaseous environmental on micro/nano structure and ambient temperature [8-18]. An advanced method for producing nano-structured materials have been developed by performing pulsed laser ablation of gold plate in super critical CO₂ [9].

One of these methods is laser induced ablation [9-16]. Different nano-wires have been synthesized by laser ablation; one of them is pig – tailed ZnO with diameter less than 100 nm in diameter at hexagonal top of nano-rods. Another is a ZnO nano – Cone with bottom diameter of 500 nm and height of 2 m on other hand complete layers of amorphous HALO layer synthesized by chemical vapor deposition (CVD) transformation into nano-crystalline Al-Al₂O₃ had been proposed for layer radiation.

Also, the surface morphology and distributions of crystalline phase of the structured samples are dependent on the layer flounce [18]. Optoelectronic materials interactions have attracted much interest among researchers because of its capabilities of unique surface modifications. Particular focus on diamond, lithium niobate, and gallium arsenide [19]. The following unique, laser assisted nano and micromachining findings were observed (1) 3D periodic nano-writing on the surface and on diamond clusters in the form of periodic

ripples shorter than laser wavelength, (2) amorphous and defective areas in the nano/sup–micrometer vicinity of laser treated region, allowing selective light trapping, and (3) surface passivation without contaminating the surface.

In this article we study the interaction of n-sec laser Nd: YAG with zinc oxide nanostructure was induced by (MPECVD).

2. Experimental

The plasma CVD system used in this study is shown in Fig.1. The plasma system consists of microwave generator operating at 2.45GHz and magnetron (Toshiba type, 2M172H AG) that was connected through a 50-Ω cable with a radiator at the center of the cylindrical waveguide (diameter = 9.6cm, length =12cm). The guided radiation power was fed into the plasma stainless-steel chamber (diameter = 10cm; length =6cm). A Zinc Chloride powder (ZnCl₂) was put in molybdenum (Mo) boat inside the center of the chamber. The substrate–target position was 45° with chamber wall inside the waveguide. The plasma spectra were collected during the deposition by an optical system into optical spectrometers (H20 monochrometer from HORBIA, Jobin-Yvon).

The chamber was evacuated by a rotary pump (CIT) Alcatel (2002B) and then subsequently argon and hydrogen gases were introduced into the chamber at different ratios. The applied microwave power was varied from 50 to 450 W. The measurement of plasma spectra have been carried out over the pressure range from 2 to 18 torr. The plasma temperature was estimated to be 7 eV as measured by the author [20]. Plasma reaction is totally isolated from the chamber walls as shown in Fig.2.

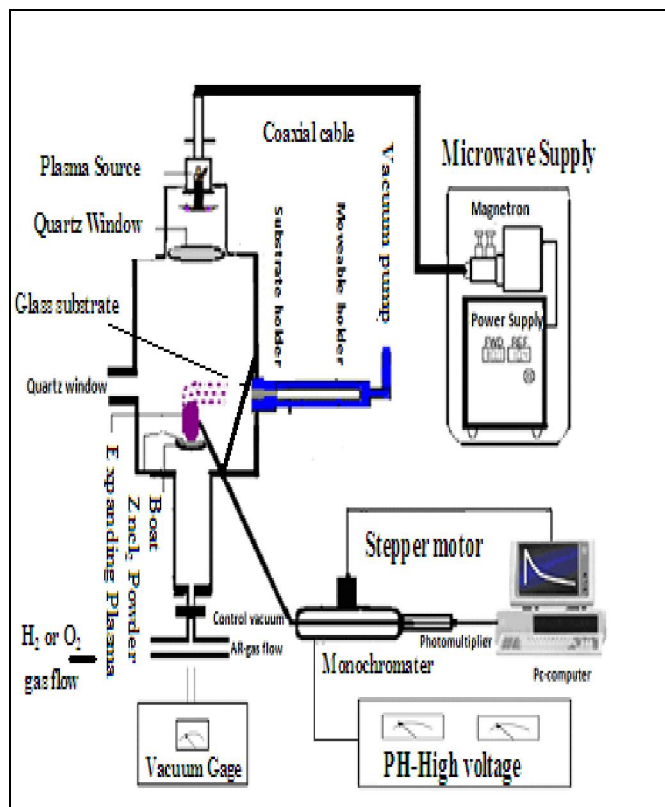


Fig.1. Low pressure Microwave plasma-Chemical Vapor Deposition (LPMP CVD) Set up.

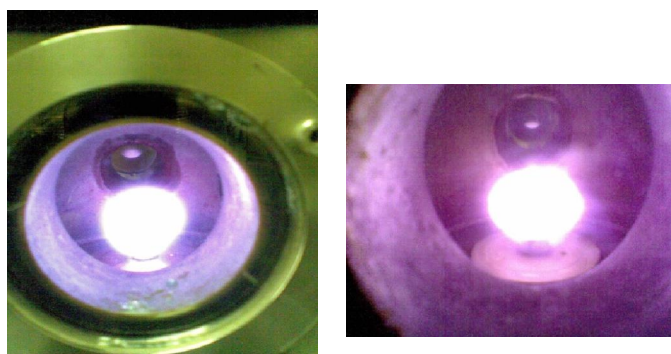


Fig.2. Induced hydrogen plasma photograph taken during deposition (a) at applied power of 100 W, (b) at applied power of 300 W.

Table (1)*

Sample	Hydrogen gas pressure	Argon gas pressure	Total pressure	Microwave power
S1	3 torr	1 torr	4 torr	250 watt
S2	5 torr	2 torr	7 torr	300 watt
S3	6 torr	2 torr	8 torr	300 watt

*the process voltage and the deposition time were 700V and 30 minutes respectively for the all

The deposition time was set to 30 min for each process. After that time, the microwave plasma power was switched off and the H₂ flow was cut off

then the system was left for 15 min to cool down to room temperature with a gas flow of argon at 3 torr. The ZnO thin film was deposited on the upper side of the glass substrate at different ratios of hydrogen and argon gas pressures.

The preparation conditions of the three samples used in this work were tabulated in table 1.

3. Optical Properties Of The Crystalline Zinc Oxide Thin Film

The absorption coefficient α of the ZnO film was determined from transmittance measurements. The energy gap (E_g) is estimated by assuming a direct

transition between valance and conduction bands using the following [13].

$$ahv = k (hv - E_g)^{1/2} \quad (2)$$

Where k is a constant, E_g is determined by extrapolating the straight line portion of the spectrum $ahv = 0$.

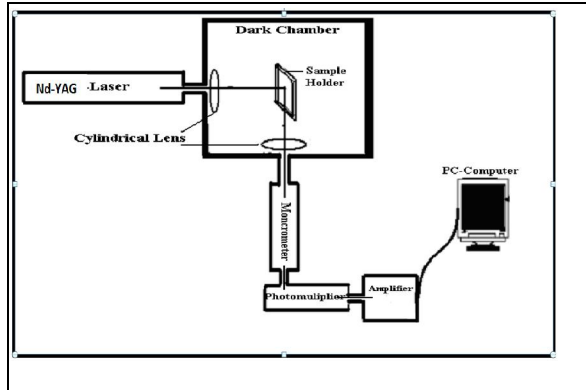


Fig.3. the laser block diagram for radiation set-up

Figure 5 shows the relation between $h\nu$ and $(ah\nu)^2$ at different partial pressure gas ratio of hydrogen: argon, (a) 3 torr:1 torr and (b) 5 torr:2 torr. The calculated E_g in both cases are 2.95 and 3.1 eV respectively. It is clear that the value of E_g show a slight dependence on the gas ratio. The energy gap have been measured using absorption system and the relation between photon energy and the coefficient as a function of wave length is showing in the following fig (2).

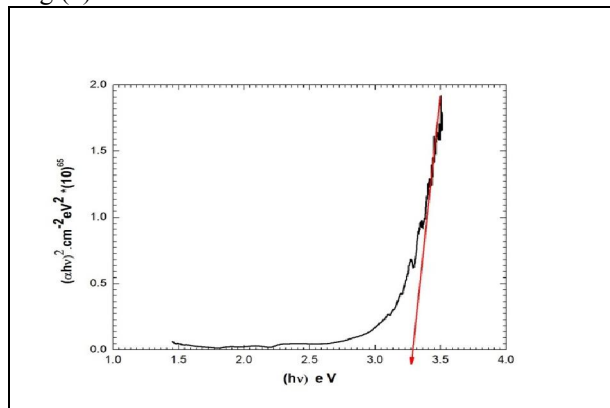


Fig.5. Measurement of energy gap for ZnO thin film prepared with gas mixture (after laser shots.)

3. X-ray Diffraction:

The X-ray diffraction (XRD) analysis of the deposited ZnO–thin film were performed using a X' Pert Pro system with Cu- $K\alpha$ radiation ($\lambda = 1.54060 \text{ \AA}$), operated at 40 kV and 40 mA. Fig.3. shows a typical XRD pattern of the ZnO nano-crystals on glass substrate for three different gas ratios of hydrogen to argon. The three gas ratio are (3 torr: 1 torr), S1, (5 torr: 2 torr), S2, and (6 torr: 2 torr) S3

with a total ambient gas pressure of 4, 7 and 8 torr respectively. The x-ray diffraction spectrum for the crystalline ZnO thin film shown in Fig.4 indicates that the film has polycrystalline nature. The x-ray diffraction a slight dependence on the gas ratio. The behaviors reveals are depend on laser shots.

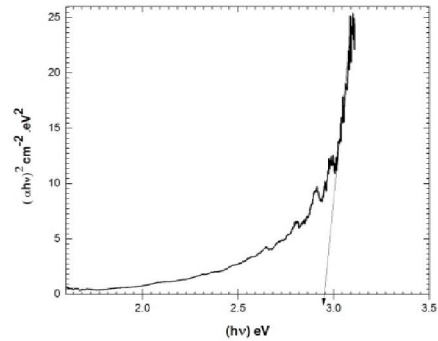


Fig.6. Measurement of energy gap for ZnO thin film prepared with gas mixture (before laser shots)

The comparison of x-ray diffractions patterns are shown, before and after radiation shots as in fig. (4).

The X-ray diffraction (XRD) analysis of the deposited ZnO–thin film were performed using a X' Pert Pro system with Cu- $K\alpha$ radiation ($\lambda = 1.54060 \text{ \AA}$), operated at 40 kV and 40 mA. Fig.3. shows a typical XRD pattern of the ZnO nano-crystals on glass substrate for three different gas ratios of hydrogen to argon. The three gas ratio are (3 torr: 1 torr), S1, (5 torr: 2 torr), S2, and (6 torr: 2 torr) S3 with a total ambient gas pressure of 4, 7 and 8 torr respectively. The x-ray diffraction spectrum for the crystalline ZnO thin film shown in Fig.4 indicates that the film has polycrystalline nature. The x-ray diffraction patterns of the crystalline ZnO reveal the existence of a ZnO single-phase with a hexagonal wurtzite structure.

In Fig.4. XRD diffraction peaks at 31.6, 34.4, 47.9, and 57.2 correspond to (100), (002), (102) and (110) plans respectively. The crystal structure of grown ZnO nanorods corresponds to hexagonal structure.

The XRD patterns consist of a (100) main peak. The full width at half maximum (FWHM) of (100) peak was $0.138 2\theta$ for the crystalline ZnO thin film. Another major orientation present is (102), while other orientation is like (002), and (110) are also seen with comparatively lower intensities which indicate that samples S1, S2, and S3 are composed of pure ZnO nanorods as agreed with other studies [22, 24, 25]. The sharp diffraction peaks confirm the high crystallinity of the synthesized nanoparticles.

Table 1. Average grain size

(hkl)	Pos. [2θ]	Height [cts]	FWHM [2θ]	d-spacing Å	Rel.Int. [%]	Grain size (nm)
(100)	22.5350	38.74	0.1574	3.94563	100.00	52
(002)	33.4191	14.70	0.1525	2.68133	37.94	55
(102)	37.8028	7.13	0.3600	2.37987	18.41	24
(110)	46.0246	10.53	0.2880	1.97043	27.18	30
Average grain size						40

The grain size of the crystallites was calculated using the well-known standard Scherer's formula [13].

$$g = \frac{0.9\lambda}{\beta \cos\theta} \quad (1)$$

4. Scanning electron microscope (SEM):

The morphology of the so-obtained crystalline zinc oxide thin films was studied with scanning electron microscopy (SEM). Figures 6, 7, and 8 show high resolution SEM images of samples S1, S2, and S3 respectively. The SEM images were taken using scanning Electron Microscope (SEM) model Quanta FEG 250 attached with EDX unit, at accelerating voltage of 200 V-30 kV, and magnification of 14 x up to 1,000,000 x.

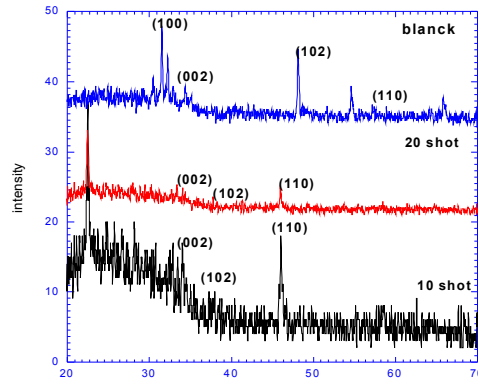
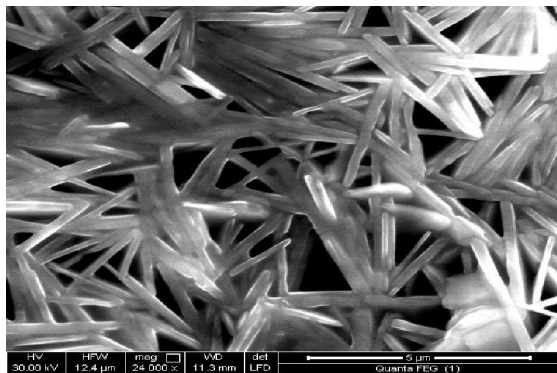
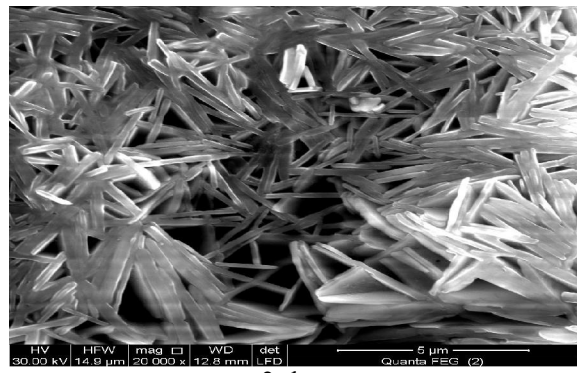


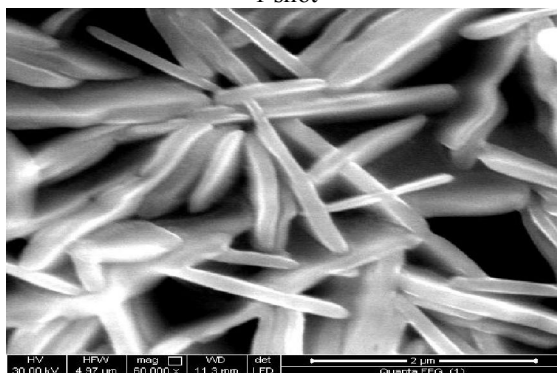
Fig. 4. XRD patterns of the ZnO thin films for three samples prepared at three different gas mixture of hydrogen and argon partial gas pressure ratio (3:1), S2 (5:2), S3 (6:2) for samples S1, S2 and S3 respectively.



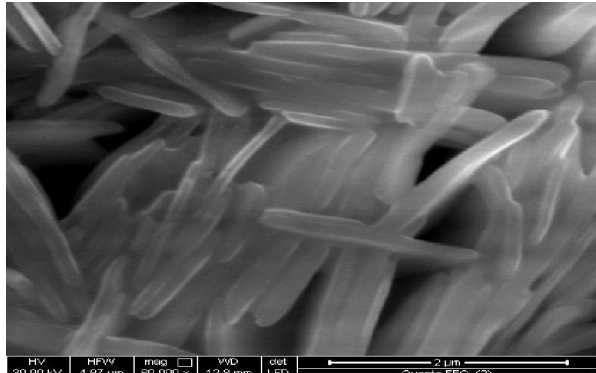
1 shot



2 shot



2 shot



10 shot

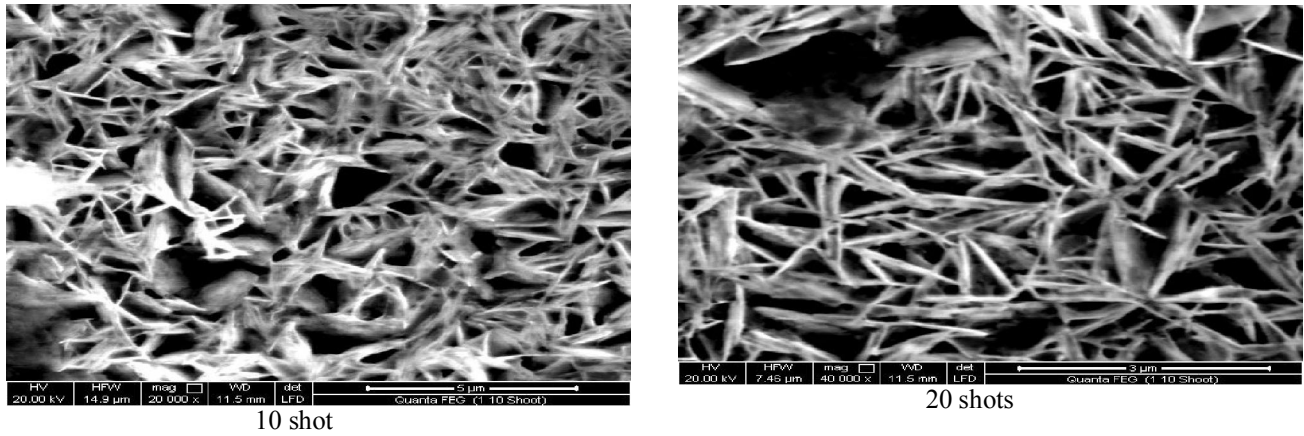
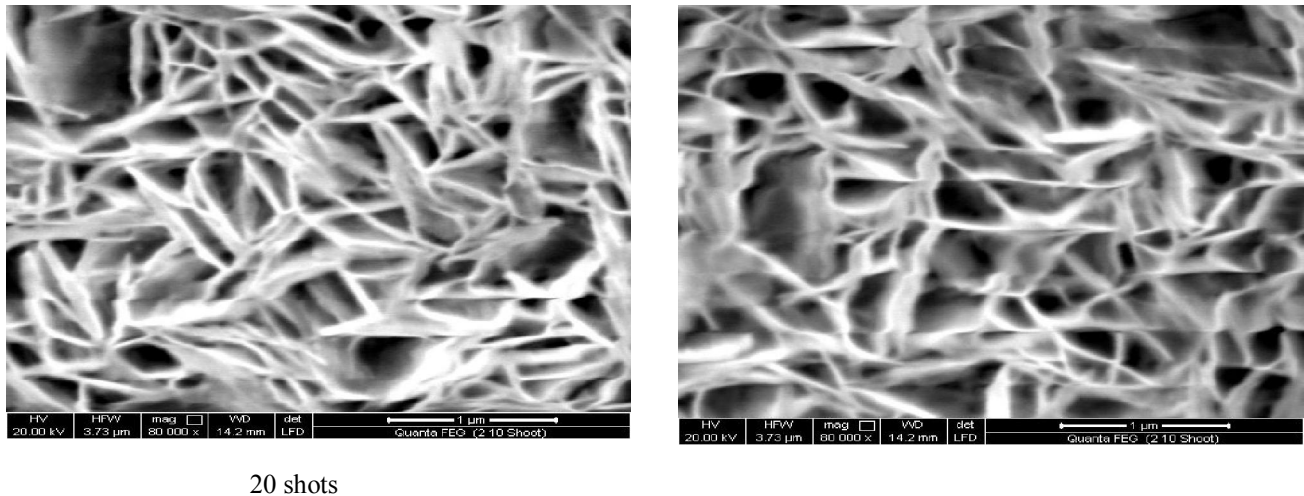


Fig.6. the SEM photographs with different magnified for (a) blank sample and (b) irradiant at different laser shots



5. Conclusion

Laser interactions shows a strong depends on the number of shots with fixing the flounce at 197 mJ. First single shot ablate nano- partical for the surface keeping the strongly coupled nano-rods giving the orthogonal shapes with common origin increasing laser shots the surface nano-tube joined together for mish shape. Also the laser shot reduced the nano-size from 80-30 nm.

Theis behaviors associated with reductions of crystalline plane corresponding to ZnO at (110) .with presence of x-ray patterns at lower angle (22.5) which indentified as zirconium oxide fluoride. The energy gap measurement reveal depends on laser shot which induced approximately changes from 3-3.25 eV

Acknowledgement

The authors are very grateful to the international Bureau KFA, Julich, Germany, for supporting the laboratory with instrumentation used in carrying out this study.

References

1. GuoshengZ., P. Fauchet, A. Siegman. Growth of spontaneous periodic surface structures on solids during laser illumination. *Phys Rev B*, 26 (1982), pp. 5366–5381
2. Siegman A., P. Fauchet. Stimulated wood’s anomalies on laser- illuminated surfaces. *IEEE J Quantum Electron*, 22 (1986), pp. 1384–1403
3. SipeJ.E., J.F. Young, J.S. Preston, H.M. van Driel. Laser induced periodic surface structure. I. *Theory Phys Rev B*, 27 (1983), pp. 1141–1154
4. Young J., J. Preston, H. van Driel, J. Sipe. Laser-induced periodic surface structure. II. Experiments on Ge, Si, Al and brass. *Phys Rev B*, 27 (1983), pp. 1155–1172
5. Borowiec A., H.K. Haugen. Subwavelength ripple formation on the surfaces of compound semiconductors irradiated with femtosecond laser pulses *Appl Phys Lett*, 82 (2003), pp. 4462–4464
6. Yasumaru N., K. Miyazaki, J. Kiuchi. Femtosecond-laser-induced nanostructure

- formed on hard thin films of TiN and DLC. *Appl Phys A*, 76 (2003), pp. 983–985
7. Barada K. Nayak, Mool C. Gupta. Ultra laser-induced self-organized conical micro/nano surface structures and their origin. *Optics and laser in Engineering* 48 (2010) 966-973.
 8. Barada K. Nayak, Mool C. Gupta. self-organized micro/nano in metal surface by ultrafast laser irradiation. *Optics and Engineering* 48 (2010) 940-949.
 9. Siti Machmudah, Wahyudiono, Yutaka Kuwahara, Mitsuru Sasaki, Motonobu Goto. Nano-structured particles production using pulsed laser ablation of gold plate in supercritical CO₂. *Journal of Supercritical Fluids* V. 60, December 2011, PP. 63–68.
 10. Shamim Ahsan Md., Farid Ahmed, Yeong Gyn Kim, Man Seop Lee, Martin B.G. Jun. Colorizing stainless steel surface by femtosecond laser induced micro/nano- structures. *Applied surface science* 257 (2011) 7771-7777.
 11. Okada T., K. Kawashima, Y. Nakata. Nano-wire pig-tailed ZnO nano-rods synthesized by laser ablation. *Thin Solid Films* Vo. 506–507, 26 May 2006, PP. 274–277.
 12. Yoshie Ishikawa, Yoshiki Shimizu, Takeshi Sasaki, Naoto oshizaki. Preparation of zinc oxide nano rods using pulsed laser ablation in water media at high temperature. *Journal of Colloid and Interface Science* Vol. 300, Issue 2, 15 August 2006, PP. 612–615.
 13. Okada T., J. Suehiro. Synthesis of nano-structured materials by laser-ablation and their application to sensors. *Applied Surface Science* Vol. 253, Issue 19, 31 July 2007, PP. 7840–7847.
 14. Hai-Li YU, ZHANG Wen-Gong. Blue fluorescence of decorated nano zinc oxide/polystyrene hybrid thin film prepared by pulsed laser ablation. *Materials letters*, 2008, vol. 62, no27, pp. 4263-4265.
 15. Bashir S., M.S. Rafique, W. Husinsky. Surface topography (nano-sized hillocks) and particle emission of metals, dielectrics and semiconductors during ultra-short-laser ablation: Towards a coherent understanding of relevant processes. *Applied Surface Science* Vol. 255, Issue 20, 30 July 2009, PP. 8372–8376.
 16. Jen-Hong, Jehnming Lin. An investigation of the synthesis of metallic nano-particles by laser ablation. *surface & coating technology* 202 (2008) 6136-6141.
 17. Benoit Delobelle, Francois Courvoisier, Patrick Delobelle. Morphology study of femtosecond laser nano-structured borosilicate glass using atomic force microscopy and scanning electron microscopy. *Optics and laser in Engineering* 48 (2010) 616-625.
 18. Petersen C, A. Lasagni, C. Holzapfel, C. Daniel, F. Mucklich, Veith. SEM/TEM characterization of periodical novel amorphous /nano-crystalline micro-composites obtained by laser interference structuring: the system HAIO-Al₂O₃. *Applied surface science* 253 (2007) 8022-8027.
 19. Ajay Malshe, Devesh Deshpande. Nano and microscale surface and sub-surface modifications induced in optical materials by femtosecond laser machining. *Journal of materials processing technology* 149 (2004) 585-590.
 20. Ismail L. Z. and A. A. EL Magd, “Pressure Dependence of the Electrical Potential and Electron Temperature Plasma,” *IEEE Transactions on Plasma Science*, vol.20, no.2, 1992.

10/12/2012